

to be less than expected for the number of backscatterers present, resulting in the calculation of coordination numbers that are too low.

The coordination numbers for the Mo edge data are rather similar, showing differences of only 10–15% (except for the Mo–Se term of peak I of $\text{Ti}_2\text{Mo}_6\text{Se}_6$, which is subject to parameter correlation in the curve-fitting procedure). The calculated coordination numbers for the Se edge show substantially more variation, ca. 30%. Formation of individual $(\text{Mo}_3\text{Se}_3)^{\frac{1}{2}}$ strands should result in a decrease in the coordination numbers for peaks II and III for $\text{Li}_2\text{Mo}_6\text{Se}_6/\text{PC}$ vs. $\text{Li}_2\text{Mo}_6\text{Se}_6$, if interchain contacts contribute appreciably to the EXAFS. Instead, however, a very slight increase in the coordination numbers is actually observed.

Conclusions

The lack of major differences between the EXAFS spectra of $\text{Li}_2\text{Mo}_6\text{Se}_6$ and $\text{Li}_2\text{Mo}_6\text{Se}_6/\text{PC}$ indicates that the Se and Mo environments in the samples are indistinguishable. Analysis of the Mo and Se EXAFS shows that both are dominated by *in-train* scattering interactions; consequently, the structure of the $(\text{Mo}_3\text{Se}_3)^{\frac{1}{2}}$ chain is not observed to be perturbed significantly upon dissolution. *Interchain* interactions make only a relatively minor contribution to the Se and Mo EXAFS, and no significant changes attributable to these contacts were observed. These results are consistent with previous TEM studies, which have demonstrated that $\text{Li}_2\text{Mo}_6\text{Se}_6$ in propylene carbonate forms bundles of one-dimensional chains whose diameter decreases with increasing

dilution. Within the concentration range amenable to study by EXAFS spectroscopy, these bundles are of sufficiently large diameter ($\geq 20 \text{ \AA}$) that the bulk of the material lies in the interior of the bundle in an environment very similar to that of the crystalline phase. The fraction of the material on the surface of the bundle and in direct contact with the solvent is small and does not make an observable contribution to the EXAFS. Despite the complexity of the system and the presence of multiple contributions to the EXAFS, analysis of the data yielded average bond distances in good agreement with X-ray results for $\text{Ti}_2\text{Mo}_6\text{Se}_6$.

Acknowledgment. This research was supported in part by the National Science Foundation—Solid State Chemistry—Grant DMR-8313252 (D.A.H. and B.A.A.). We thank the staff at CHESS and S. M. Kauzlarich for their assistance and the following people for their help in collecting the data: M. R. Antoni, S. Burman, W. Frazier, O. Fussa, C. L. Hulse, J. Orlando, and T. Zirino.

Registry No. $\text{Li}_2\text{Mo}_6\text{Se}_6$, 92341-41-8; $\text{In}_2\text{Mo}_6\text{Se}_6$, 75036-77-0; $\text{Ti}_2\text{Mo}_6\text{Se}_6$, 73667-07-9; Mo, 7439-98-7; Se, 7782-49-2; propylene carbonate, 108-32-7.

Supplementary Material Available: Figures of background-removed EXAFS ($k^3[\chi(k)]$ vs. k) from Mo and Se edges of $\text{Li}_2\text{Mo}_6\text{Se}_6$, $\text{Li}_2\text{Mo}_6\text{Se}_6/\text{PC}$, $\text{In}_2\text{Mo}_6\text{Se}_6$, and $\text{Ti}_2\text{Mo}_6\text{Se}_6$ and tables of parameters (r , ΔE , σ , B) determined from curve fitting of the theoretical EXAFS equation to filtered data of Mo and Se edge EXAFS (11 pages). Ordering information is given on any current masthead page.

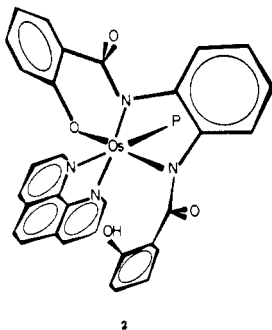
Contribution No. 7439 from The Chemical Laboratories, California Institute of Technology, Pasadena, California 91125

A Novel Nonplanar Amido-*N* Ligand Type. Nonplanarity in the Amido-*N* Ligand Induced by Steric Effects

Terrence J. Collins,*¹ Ting Lai, and Geoffrey T. Peake

Received November 19, 1986

The X-ray crystal structure of $\text{Os}(\eta^3\text{-}(\text{H})\text{HBA-B})(\text{PPh}_3)(\text{phen})$ (**2**; the free-base ligand is $\text{H}_4\text{HBA-B}$ = 1,2-bis(2-hydroxybenz-amido)benzene; phen = 1,10-phenanthroline), an osmium(III) complex containing a tridentate phenolato-diamido-*N* ligand, is reported. Crystal data: $\text{OsC}_{50}\text{H}_{35}\text{N}_4\text{O}_4\text{P}\cdot 2\text{C}_2\text{H}_5\text{OH}$, $a = 10.448$ (4) Å , $b = 14.454$ (6) Å , $c = 16.598$ (7) Å , $\alpha = 89.27$ (3)°,



$\beta = 99.74$ (3)°, $\gamma = 111.44$ (3)°, $V = 2296$ (1) Å^3 , triclinic, $P\bar{1}$, $Z = 2$, $R(I > 0) = 0.054$ (7897 reflections), $R(I > 3\sigma(I)) = 0.047$ (6986 reflections). This molecule contains the first member of a new class of nonplanar amido-*N* ligands where the nonplanarity can be attributed to steric effects. The amido-*N* ligand with the uncoordinated hydroxybenzoyl arm is distinctly nonplanar with a τ value (a twist angle about the C–N bond) of -40° . The χ_N value (an angle reflecting pyramidal distortion at N) of -49° is the largest for any organic amido-*N* ligand, and the χ_C value of -10° is as large as any that have been observed previously.

Introduction

We have recently reported the first cases of nonplanar organic amido-*N* ligands with large twist angles about the C–N bond.² The twisting can be quantified by the angle τ , which approximates the smaller angle between the carbonyl carbon and the nitrogen

parent $p\pi$ orbitals (Figure 1).² Of the 120 structurally characterized cases of monodentate metallo-amido-*N* groups derived from parent mono-*N*-substituted amides, only nine have τ values greater than 10° . The known cases are confined to complexes of polyanionic chelating (PAC) ligands of the type described here. Two distinct classes of complexes of nonplanar amido-*N* ligands, distinguished by the nature of the primary cause of the nonplanarity, have already been identified: (i) in class I complexes, nonplanar amido-*N* ligands are formed because nonplanar amido-*N* ligands are thermodynamically favored over planar analogues

- (1) Alfred P. Sloan Research Fellow, 1986–1988; Dreyfus Teacher-Scholar, 1986–1990.
 (2) Collins, T. J.; Coots, R. J.; Furutani, T. T.; Keech, J. T.; Peake, G. T.; Santarsiero, B. D. *J. Am. Chem. Soc.* **1986**, *108*, 5333–5339.

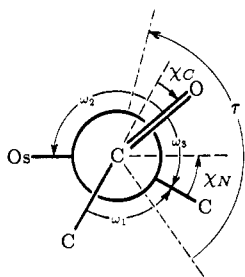


Figure 1. Parameters for describing bond angles in metallo-amido-*N* groups, where $\bar{\tau} = \tau \bmod \pi$.

accessible by isomerization at the metal center.^{2,3} This class is without precedent in amide chemistry. (ii) In class II complexes, structural constraints of the coordination sphere force the formation of nonplanar amido-*N* ligands.^{2,3} This second class contains the inorganic counterparts of certain constrained organic amide functional groups, the major class of nonplanar amides in organic chemistry.² Here we describe the first example of a third inorganic class; a PAC-ligand complex containing a distinctly nonplanar amido-*N* ligand in which steric effects can be identified as the principal cause of the nonplanarity.

Experimental Section

Materials. Acetone (Mallinckrodt), benzene (thiophene free, Aldrich), diethyl ether (Baker), and ethanol (USI) were reagent grade and were used as received, unless otherwise noted. Dichloromethane (Baker) was distilled from calcium hydride prior to use. Acetic acid (Mallinckrodt), 4-(dimethylamino)pyridine (Aldrich), 1,10-phenanthroline (phen, Aldrich), pyridine (Aldrich), and triethylamine (reagent MCB) were all used as received. The synthesis of *trans*-Os(η^4 -HBA-B)(PPh₃)₂ has been described elsewhere.³ The silica gel used in column chromatography was 60–200 mesh (Davison).

Syntheses. Os(η^3 -(H)HBA-B)(PPh₃)(phen) (**2**).⁴ *trans*-Os(η^4 -HBA-B)(PPh₃)₂ (1 1.00 g, 0.944 mmol) was dissolved in CH₂Cl₂ (110 mL), and 1,10-phenanthroline (200 mg, 1.11 mmol) was added. The solution was stirred at room temperature (30 min). Ethanol was added, and the product crystallized upon removal of CH₂Cl₂. The brown crystals were collected, washed with ethanol and diethyl ether, and dried under vacuum; yield 846 mg (92%). IR (cm⁻¹, Nujol mull): broad-structured bands in ν_{CO} (amide) region at 1570, 1580, 1596, 1613 (region complicated by bands of aromatic ligands). The solution IR spectrum (CHCl₃) shows no major differences. Anal. Calcd for C₅₀H₃₅N₄O₄OsP: C, 61.40; H, 3.71; N, 5.73. Found: C, 60.95; H, 3.86; N, 5.54.

Os(η^3 -(CH₂CO)HBA-B)(PPh₃)(phen) (**3**). Os(η^3 -(H)HBA-B)(PPh₃)(phen) (50 mg, 1.1 μ mol) was dissolved in CH₂Cl₂ (10 mL). 4-(Dimethylamino)pyridine (5 mg, 41 μ mol), triethylamine (1 mL), and acetic anhydride (1.5 mL) were added. The solution was stirred at room temperature (20 min). The volatiles were removed on a rotary evaporator, and the residue was dissolved in a small volume of CH₂Cl₂. The mixture was purified by passage down a silica gel column (10 cm \times 2 cm) by elution first with CH₂Cl₂ to remove organic impurities and then with 3:2 CH₂Cl₂-acetone to remove the brown product, which was crystallized from benzene-diethyl ether; yield 35 mg (67%). IR (cm⁻¹, Nujol mull): 1767 (m, ν_{CO} (ester)), 1600 (s, ν_{CO} (amide)). Anal. Calcd for C₅₂H₃₈N₄O₅OsP₂C₆H₆: C, 63.43; H, 4.04; N, 5.10. Found: C, 63.44; H, 4.11; N, 5.09.

Electrochemistry. Dichloromethane used in cyclic voltammetric experiments was reagent grade and was further purified by distillation from calcium hydride. TBAP (tetrabutylammonium perchlorate, Southwestern Analytical Chemicals) supporting electrolyte was dried, recrystallized twice from acetone-diethyl ether, and then dried in vacuo. The TBAP concentration in all experiments was 0.1 M. BPG (basal plane graphite) electrodes (Union Carbide Co., Chicago) used for cyclic voltammetry were cut and mounted as previously described.⁵ The reference electrode was a saturated KCl silver-silver chloride electrode (Ag-AgCl). In all experiments ferrocene was added at the conclusion of the experiment as an internal potential standard.

Cyclic voltammetry was performed with a Princeton Applied Research Model 173/179 potentiostat-digital coulometer equipped with positive-feedback *iR* compensation and a Model 175 universal programmer.

Table I. Experimental Data for the Structure Determination of Os(η^3 -(H)HBA-B)(PPh₃)(phen) (**2**)

formula	OsC ₅₀ H ₃₅ N ₄ O ₄ P ₂ C ₂ H ₅ OH
fw	1069.2
unit cell constants	$a = 10.448$ (4) Å, $b = 14.454$ (6) Å, $c = 16.598$ (7) Å, $\alpha = 89.27$ (3)°, $\beta = 99.74$ (3)°, $\gamma = 111.44$ (3)°, $V = 2296$ (1) Å ³
D_{calcd} ($Z = 2$)	1.546 g cm ⁻³
space group	$P\bar{1}$
cryst size	0.26 \times 0.39 \times 0.45 mm
μ (Mo K α)	30.4 cm ⁻¹
scan type and speed	θ - 2θ , 4° min ⁻¹
scan range	1° below K α_1 to 1° above K α_2
bkgd counting	stationary counts for half of scan time at each end of scan
collecn range	$\pm h, \pm k, l$, $4 < 2\theta < 50$; $\pm h, \pm k, -l$, $4 < 2\theta < 40$
no. of reflcns measd	13 395
no. of unique data, m	8145
no. of data with $I > 0$	7897
no. of data with $I > 3\sigma(I)$	6986
no. of parameters refined, p	596
R^a (for $I > 0$)	0.054
R (for $I > 3\sigma(I)$)	0.047
goodness of fit ^b	2.90

^a $R = \sum ||F_o| - |F_c|| / \sum |F_o|$. ^b Goodness of fit = $[\sum (F_o^2 - F_c^2)^2 / (m - p)]^{1/2}$.

Current-voltage curves were recorded on a Houston Instruments Model 2000 X-Y recorder. Plots of peak current vs. the square root of scan rate over the range 20–500 mV s⁻¹ were made and found to be linear for couples that are stated to be reversible.

X-ray Data Collection and Structure Determination of *trans*-Os(η^3 -(H)HBA-B)(phen)(PPh₃). A crystal of *trans*-Os(η^3 -(H)HBA-B)(phen)(PPh₃) was obtained from a CH₂Cl₂-EtOH solution. Intensity data were collected on a Nicolet P2₁ diffractometer using the θ - 2θ scanning technique. Three check reflections, monitored every 100 data measurements, showed a decrease in intensity of about 2% during the 250 h of X-ray exposure. The intensities were corrected for a linear decay and reduced to $|F_o|$'s. Multiple observations were averaged to yield 8145 independent reflections. We estimate the range of transmission factors to be about 0.15–0.18. No absorption correction was applied.

The positions of the osmium and phosphorus atoms were obtained from a three-dimensional Patterson function, and the rest of the non-hydrogen atoms were recovered from subsequent Fourier and difference Fourier syntheses. The R factor was 0.25.

Refinement was carried out by full-matrix least-squares methods. The quantity minimized was $\sum w(F_o^2 - F_c^2)^2$, with weight $w = 1/\sigma^2(F_o^2)$. Atomic scattering factors with the real part of anomalous dispersion applied for osmium and phosphorus were obtained from ref 9. Calculations were carried out on a VAX 11750 computer using the CRYM system.

After several cycles of least-squares adjustment of the coordinates for all non-hydrogen atoms, anisotropic thermal parameters for osmium and phosphorus, and isotropic thermal parameters for the rest, the R factor was reduced to 0.066. At this stage all hydrogen atoms, except those attached to oxygen atoms, were inserted in their calculated positions with assigned isotropic thermal parameters the same as those of their parent carbon atoms. During the last four cycles a list of 596 parameters was adjusted: atomic coordinates and anisotropic thermal parameters of all the non-hydrogen atoms, a scale factor, and a secondary extinction coefficient. Atomic coordinates of all except the solvent atoms were kept in one matrix, the scale factor, the secondary extinction coefficient, and the anisotropic thermal parameters of all except the carbon atoms in the triphenylphosphine group of the osmium complex in a second matrix, and the rest of the parameters in a third matrix. Parameters of the hydrogen atoms were not refined.

The final R index for 7897 reflections was 0.054, and the final value of the secondary extinction parameter was $(0.26 \pm 0.03) \times 10^{-7}$. A summary of experimental data is included in Table I.

Results and Discussion

Complex **2** can be synthesized easily from the osmium(IV) complex **1** (Scheme I). The formulation of **2** as an osmium(III) complex rests on the following evidence. The solid-state room-temperature magnetic moment is 1.38 μ_B . The cyclic voltammogram of **2** reveals one reversible reduction at -1.11 V (vs. Fc^{+/}Fc), one reversible oxidation at -0.31 V, and a nonreversible

(3) Anson, F. C.; Collins, T. J.; Gipson, S. L.; Keech, J. T.; Krafft, T. E.; Peake, G. T. *J. Am. Chem. Soc.* **1986**, *108*, 6593–6605.

(4) Ligand name: H₄HBA-B = 1,2-bis(2-hydroxybenzamido)benzene.

(5) Oyama, N.; Anson, F. C. *J. Am. Chem. Soc.* **1979**, *101*, 3450–3456.

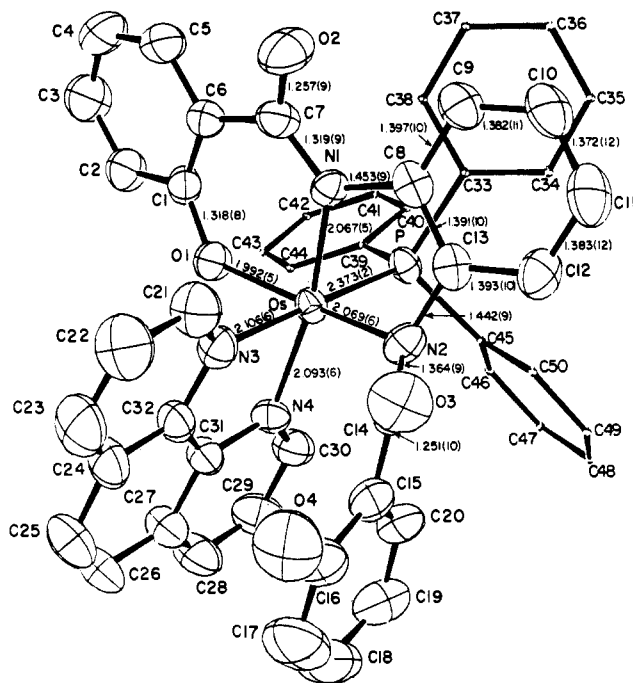
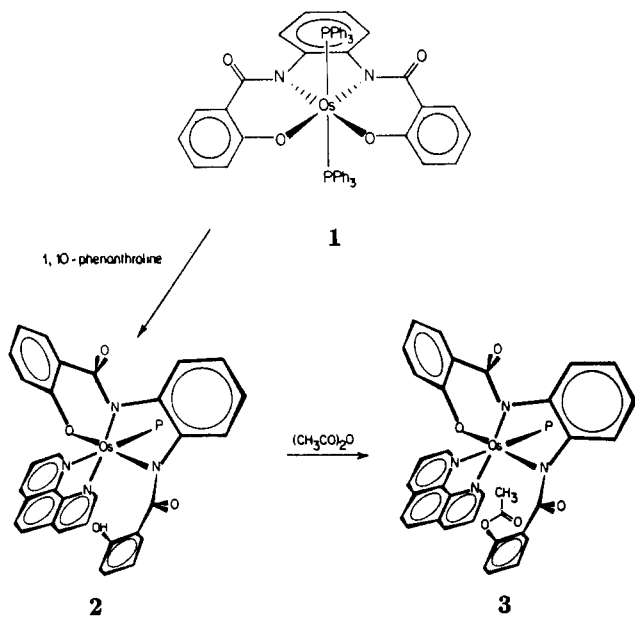


Figure 2. Molecular structure of $\text{Os}(\eta^3\text{-(H)HBA-B})(\text{PPh}_3)(\text{phen})$ (**2**).

Scheme I



oxidation at +0.72 V. On the basis of the direct spectroscopic evidence, an osmium(IV) phenoxide zwitterion is difficult to rule out, i.e. a structure that differs from the proposed formulation by removing the hydrogen atom from the phenol oxygen. No distinctive ν_{OH} band can be located in the IR spectrum; H-bonding with the amide oxygen is expected, and the intramolecular O(3)–O(4) distance of 2.58 (1) Å is consistent with such bonding.⁶ However, the electrochemical data strongly support the osmium(III) formulation; we would expect oxidation of an osmium(IV)–phenoxide zwitterion to occur at a potential at least 1 V positive of that observed.^{3,7} Further support for the osmium(III) formulation has been obtained by treating **2** with acetic anhydride to give the monoacetylated product, which remains neutral as

Table II. Selected Bond Lengths and Angles for $\text{Os}(\eta^3\text{-(H)HBA-B})(\text{PPh}_3)(\text{phen})$ (**2**)

Os–P	2.372 (2)	Os–N1	1.922 (5)
Os–N1	2.067 (5)	Os–N2	2.069 (6)
Os–N3	2.106 (6)	Os–N4	2.093 (6)
P–C33	1.838 (7)	P–C39	1.836 (7)
P–C45	1.832 (7)	O1–C1	1.318 (8)
O2–C7	1.257 (9)	O3–C14	1.251 (10)
O4–C16	1.352 (11)	N1–C7	1.319 (9)
N1–C8	1.453 (9)	N2–C13	1.442 (9)
N2–C14	1.364 (9)	N4–C30	1.339 (9)
N3–C32	1.364 (9)	N3–C21	1.325 (10)
N4–C31	1.374 (9)	C1–C2	1.413 (11)
C1–C6	1.410 (10)	C2–C3	1.352 (12)
C3–C4	1.401 (14)	C4–C5	1.381 (13)
C5–C6	1.386 (11)	C6–C7	1.513 (10)
C8–C9	1.397 (10)	C8–C13	1.391 (10)
C9–C10	1.382 (11)	C10–C11	1.372 (12)
C11–C12	1.383 (12)	C12–C13	1.393 (10)
C14–C15	1.477 (11)	C15–C16	1.405 (12)
C15–C20	1.381 (13)	C16–C17	1.400 (14)
C17–C18	1.35 (2)	C18–C19	1.394 (15)
C19–C20	1.381 (13)		
O1–Os–P	95.57 (14)	N1–Os–P	89.3 (2)
N2–Os–P	95.1 (2)	N3–Os–P	178.4 (2)
N4–Os–P	99.89 (2)	N1–Os–O1	90.8 (2)
N2–Os–O1	166.3 (2)	N3–Os–O1	84.1 (2)
N4–Os–O1	82.9 (2)	N2–Os–N1	80.7 (2)
N3–Os–N1	92.3 (2)	N4–Os–N1	169.4 (2)
N3–Os–N2	85.5 (2)	N4–Os–N2	103.7 (2)
N4–Os–N3	78.5 (2)	C33–P–Os	116.5 (2)
C39–P–Os	116.4 (2)	C45–P–Os	113.3 (2)
C39–P–C33	100.8 (3)	C45–P–C33	103.4 (3)
C45–P–C39	104.5 (3)	C1–O1–Os	127.1 (4)
C7–N1–Os	128.7 (5)	C8–N1–Os	111.5 (4)
C8–N1–C7	119.8 (6)	C13–N2–Os	110.1 (4)
C14–N2–Os	123.6 (5)	C14–N2–C13	114.4 (6)
C21–N3–Os	127.1 (5)	C32–N3–Os	113.6 (5)
C32–N3–C21	119.2 (6)	C30–N4–Os	129.7 (5)
C31–N4–Os	113.8 (4)	C31–N4–C30	116.2 (6)
C2–C1–O1	115.8 (6)	C6–C1–O1	125.8 (7)
C6–C1–C2	118.3 (7)	C3–C2–C1	121.9 (8)
C4–C3–C2	120.4 (9)	C5–C4–C3	118.0 (9)
C6–C5–C4	123.1 (8)	C5–C6–C1	118.2 (7)
C7–C6–C1	126.0 (7)	C7–C6–C5	115.7 (7)
N1–C7–O2	124.0 (7)	C6–C7–O2	116.4 (7)
C6–C7–N1	119.6 (7)	C9–C8–N1	126.4 (7)
C13–C8–N1	114.8 (6)	C13–C8–C9	118.6 (7)
C10–C9–C8	120.4 (7)	C11–C10–C9	120.5 (8)
C12–C11–C10	120.3 (8)	C13–C12–C11	119.5 (8)
C8–C13–N2	118.0 (6)	C12–C13–N2	121.1 (7)
C12–C13–C8	120.7 (7)	N2–C14–O3	122.7 (7)
C15–C14–O3	118.4 (7)	C15–C14–N2	118.9 (7)
C16–C15–C14	118.4 (8)	C20–C15–C14	121.9 (8)
C20–C15–C16	119.7 (8)	C15–C16–O4	122.8 (8)
C17–C16–O4	119.0 (9)	C17–C16–C15	118.2 (9)
C18–C17–C16	121.2 (10)	C19–C18–C17	120.9 (11)
C20–C19–C18	118.7 (10)	C19–C20–C15	121.2 (8)

expected for the osmium(III) formulation. We favor a formulation in which acetylation has proceeded at the phenol oxygen. As expected for this formulation, the formal potentials for the reversible couples of the acetylated product are similar to those of **2**: –1.11, –0.28 (+0.68 V, nonreversible).

The molecular structure of **2** (Figure 2, Tables I–III) has several striking features. The PAC ligand is three-coordinate with one phenolato and two amido-*N* donors. The second phenol is not coordinated. This is the first case of a three-coordinate PAC ligand of this type. The amido-*N* ligand with the attached uncoordinated phenol substituent is distinctly nonplanar; the τ value is -40° . Only five monodentate metallo-amido-*N* groups derived from parent mono-*N*-substituted amides have τ values of greater magnitude.² The χ_{N} value of -49° is the greatest in magnitude found to date.² Nine reported $|\chi_{\text{N}}|$ values are greater than 20° , and the greatest of these is 33° .² The χ_{C} value of -10° is among the largest in magnitude with only two other cases having $|\chi_{\text{C}}|$ values of 10° .² In all, only 13 cases have $|\chi_{\text{C}}|$ values greater than 5° . The cor-

(6) Pimentel, G. C.; McClellan, A. L. *The Hydrogen Bond*; W. H. Freeman: San Francisco, 1960; p 260.

(7) Anson, F. C.; Collins, T. J.; Gipson, S. L.; Keech, J. T.; Krafft, T. E.; Santarsiero, B. D.; Spies, G. H. *J. Am. Chem. Soc.* **1984**, *106*, 4460–4472.

Table III. Atom Coordinates in 2

	x	y	z		x	y	z
Os	15 141 (3)	19 195 (2)	24 227 (2)	C24	2 312 (96)	-7 979 (56)	9 584 (48)
P	29 695 (18)	32 753 (12)	33 501 (10)	C25	9 750 (120)	-14 380 (61)	8 789 (58)
O1	23 756 (45)	24 781 (31)	14 547 (27)	C26	22 951 (115)	-12 171 (62)	12 795 (58)
O2	-11 788 (57)	33 515 (44)	13 233 (34)	C27	29 976 (90)	-3 437 (55)	18 278 (49)
O3	-18 109 (54)	-1 735 (38)	30 902 (37)	C28	43 319 (101)	-1 039 (63)	22 824 (57)
O4	-15 928 (67)	-17 571 (41)	25 258 (40)	C29	48 784 (85)	7 159 (59)	28 067 (55)
N1	997 (54)	26 213 (35)	21 564 (31)	C30	41 026 (78)	12 991 (52)	28 865 (45)
N2	1 807 (55)	12 313 (38)	32 242 (32)	C31	22 858 (77)	2 817 (48)	19 274 (42)
N3	2 703 (60)	7 019 (39)	16 021 (33)	C32	9 169 (80)	617 (48)	14 798 (42)
N4	28 082 (57)	10 988 (36)	24 680 (33)	C33	22 118 (67)	41 847 (47)	35 836 (42)
C1	20 646 (73)	31 104 (47)	9 547 (40)	C34	19 720 (75)	43 424 (54)	43 541 (45)
C2	29 726 (82)	35 079 (55)	3 897 (46)	C35	13 771 (83)	50 304 (60)	44 800 (55)
C3	27 135 (103)	41 008 (65)	-2 015 (54)	C36	10 316 (90)	55 628 (61)	38 604 (63)
C4	15 076 (108)	43 308 (65)	-2 777 (51)	C37	12 824 (87)	54 212 (58)	30 919 (62)
C5	6 396 (89)	39 706 (58)	2 861 (48)	C38	18 797 (77)	47 418 (52)	29 473 (48)
C6	8 823 (74)	33 743 (48)	9 076 (41)	C39	45 934 (67)	40 984 (45)	30 384 (39)
C7	-1 384 (74)	30 983 (48)	14 988 (44)	C40	53 344 (79)	50 322 (54)	34 587 (48)
C8	-7 146 (66)	25 265 (49)	28 014 (42)	C41	65 553 (86)	56 595 (55)	32 302 (57)
C9	-14 469 (72)	31 275 (53)	29 460 (47)	C42	70 520 (80)	53 636 (62)	25 927 (54)
C10	-20 542 (78)	30 253 (61)	36 357 (51)	C43	63 650 (72)	44 574 (53)	22 031 (46)
C11	-19 639 (83)	23 213 (66)	41 819 (50)	C44	51 398 (72)	38 203 (48)	24 247 (42)
C12	-12 711 (75)	17 018 (56)	40 447 (45)	C45	35 343 (70)	28 900 (46)	43 603 (38)
C13	-6 462 (66)	18 063 (49)	33 543 (40)	C46	49 288 (77)	31 447 (58)	47 194 (45)
C14	-5 075 (79)	2 254 (51)	32 165 (44)	C47	53 015 (93)	27 943 (74)	54 537 (54)
C15	3 161 (84)	-4 224 (51)	33 356 (46)	C48	42 888 (110)	21 670 (73)	58 567 (52)
C16	-2 818 (101)	-13 888 (56)	29 705 (55)	C49	28 987 (94)	19 158 (62)	55 211 (47)
C17	5 142 (118)	-19 878 (62)	30 576 (70)	C50	25 381 (79)	22 803 (56)	47 927 (44)
C18	18 053 (125)	-16 720 (71)	35 301 (69)	C51	58 926 (204)	12 362 (153)	5 527 (127)
C19	23 742 (101)	-7 351 (66)	39 308 (57)	C52	54 296 (170)	19 362 (106)	9 015 (92)
C20	16 283 (89)	-1 147 (55)	38 176 (49)	O5	61 525 (113)	28 478 (88)	5 556 (72)
C21	-10 371 (82)	4 969 (56)	12 290 (49)	O6	52 769 (158)	75 892 (127)	14 392 (118)
C22	-17 511 (92)	-3 455 (65)	6 974 (55)	C53	29 016 (239)	64 241 (91)	13 908 (103)
C23	-11 306 (106)	-9 901 (61)	5 652 (53)	C54	45 387 (319)	66 369 (264)	15 103 (159)
H2	3 791 (0)	3 354 (0)	427 (0)	H37	1 043 (0)	5 794 (0)	2 657 (0)
H3	3 356 (0)	4 364 (0)	-564 (0)	H38	2 066 (0)	4 657 (0)	2 418 (0)
H4	1 298 (0)	4 723 (0)	-705 (0)	H40	4 997 (0)	5 228 (0)	3 899 (0)
H5	-168 (0)	4 138 (0)	247 (0)	H41	7 052 (0)	6 293 (0)	3 506 (0)
H9	-1 527 (0)	3 611 (0)	2 568 (0)	H42	7 886 (0)	5 801 (0)	2 431 (0)
H10	-2 537 (0)	3 445 (0)	3 734 (0)	H43	6 727 (0)	4 259 (0)	1 776 (0)
H11	-2 384 (0)	2 257 (0)	4 656 (0)	H44	4 664 (0)	3 182 (0)	2 149 (0)
H12	-1 223 (0)	1 207 (0)	4 419 (0)	H46	5 637 (0)	3 575 (0)	4 448 (0)
H17	156 (0)	-2 627 (0)	2 783 (0)	H47	6 262 (0)	2 982 (0)	5 688 (0)
H18	2 320 (0)	-2 098 (0)	3 590 (0)	H48	4 552 (0)	1 912 (0)	6 362 (0)
H19	3 268 (0)	-521 (0)	4 276 (0)	H49	2 198 (0)	1 490 (0)	5 796 (0)
H20	2 020 (0)	536 (0)	4 076 (0)	H50	1 575 (0)	2 113 (0)	4 573 (0)
H21	-1 497 (0)	934 (0)	1 326 (0)	H51A	5 449 (0)	594 (0)	755 (0)
H22	-2 681 (0)	-469 (0)	428 (0)	H51B	5 638 (0)	1 198 (0)	-24 (0)
H23	-1 613 (0)	-1 562 (0)	206 (0)	H51C	6 871 (0)	1 434 (0)	706 (0)
H25	537 (0)	-2 030 (0)	538 (0)	H52A	5 681 (0)	1 990 (0)	1 481 (0)
H26	2 772 (0)	-1 647 (0)	1 200 (0)	H52B	4 448 (0)	1 754 (0)	750 (0)
H28	4 855 (0)	-510 (0)	2 231 (0)	H53A	2 393 (0)	5 739 (0)	1 434 (0)
H29	5 793 (0)	890 (0)	3 120 (0)	H53B	2 736 (0)	6 800 (0)	1 803 (0)
H30	4 509 (0)	1 871 (0)	3 255 (0)	H53C	2 599 (0)	6 624 (0)	867 (0)
H34	2 215 (0)	3 980 (0)	4 797 (0)	H54A	4 690 (0)	6 252 (0)	1 097 (0)
H35	1 207 (0)	5 133 (0)	5 009 (0)	H54B	4 827 (0)	6 427 (0)	2 033 (0)
H36	616 (0)	6 026 (0)	3 953 (0)				

responding values of these parameters for the coordinated amido-*N* ligand in 2 are $\bar{\tau} = -12^\circ$, $\chi_N = -1^\circ$, and $\chi_C < 1^\circ$.

The cause of the highly unfavorable distortions in the nonplanar amido-*N* ligand of 2 appears to be a steric clash between the entire carboxyphenol *N*-substituent and the bidentate phenanthroline ligand (Figure 2). The dihedral angle between the best planes of the carboxyphenol arm and the phenanthroline group is 12° . Distances between the atoms of the carboxyphenol arm and the phenanthroline vary from 2.70 to 3.50 Å. The shorter contacts are within van der Waals distances.⁸

(8) These distances can be compared with layered trimesic acid (benzene-1,3,5-tricarboxylic acid) structures where the interlayer distances are 3.31 and 3.32 Å. Herbstein, F. H.; Marsh, R. E. *Acta Crystallogr., Sect. B: Struct. Crystallogr. Cryst. Chem.* 1977, 33, 2358-2367. The intersheet distance in β -graphite is 3.35 Å. Pauling, L. *Proc. Natl. Acad. Sci., U.S.A.* 1966, 56, 1646-1652.

(9) *International Tables for X-ray Crystallography*; Kynoch: Birmingham, England, 1974.

Conclusion

Complex 2 is the first member of a third class of inorganic compounds with nonplanar amido-*N* ligands (large $\bar{\tau}$ values). The distinguishing feature of this new class is that steric effects are the primary cause of the nonplanarity.

Acknowledgment. We thank the Rohm and Haas Co., the Atlantic Richfield Corp. of America, and the National Science Foundation (Grant CHE-84-06198) for support of this work. We extend our deep appreciation to Dr. Richard E. Marsh for many helpful discussions. Upgrade of the X-ray diffraction facility was supported by NSF Grant CHE-82-19039.

Registry No. 1, 103191-18-0; 2, 107890-97-1; 3, 107890-98-2; H₄HBA-B, 103528-00-3; acetic anhydride, 108-24-7.

Supplementary Material Available: Listings of atom coordinates and Gaussian amplitudes and of bond distances and angles (6 pages); a listing of structure factor amplitudes (31 pages). Ordering information is given on any current masthead page.